Diffusion Tensor Imaging: Reconstruction Using Deterministic Error Bounds

Yury Korolev[1], Tuomo Valkonen[2] and Artur Gorokh[3]

[1]Queen Mary University of London, UK [2]University of Cambridge, UK
[3]Cornell University, USA

SIAM Conference on Imaging Science 2016
May 23-26, 2016. Albuquerque NM, USA

Layout

Diffusion Tensor Imaging

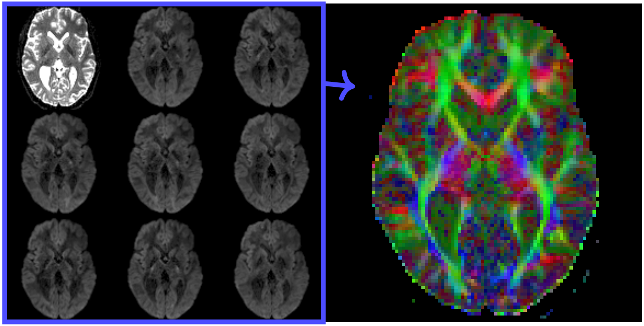

Stejskal-Tanner equation

$$s_i(x) = s_0(x) exp(-\langle b_i \otimes b_i, u(x) \rangle), \quad i = 1, \dots, n \tag{1}$$

Rician noise in the values s_i.

Reconstruction based on L_2 fidelity

- L_2 reconstruction in the non-linear model[1]

$$\min_{u\geq 0}\sum_{i=1}^{n}\|s_i - T_i(u)\|_{L_2}^2 + \alpha R(u), \tag{2}$$

where $[T_i(u)](x) := s_0(x)exp(-\langle b_i \otimes b_i, u(x)\rangle)$.

- Regression and denoising in the linearised model[2]

$$\min_{u\geq 0}\sum_{i=1}^{n}\|f - u\|_{L_2}^2 + \alpha R(u), \tag{3}$$

where each f is solved by regression for u from Eq. 1.

---

[1]Valkonen (2014). *A primal-dual hybrid gradient method for non-linear operators with applications to MRI*, Inv. Prob. 30, 055012

[2]Valkonen, Bredies, Knoll (2013). *Total generalised variation in diffusion tensor imaging*, SIAM J. Imaging Sci. 6, 487- 525

- L_2 – fidelity not fully justified in the non-linear model (2) because the noise in the data is not Gaussian (it is Rician);
- In the linearised model (3), the Gaussian noise assumption is even more removed from truth;

- L_2 – fidelity not fully justified in the non-linear model (2) because the noise in the data is not Gaussian (it is Rician);
- In the linearised model (3), the Gaussian noise assumption is even more removed from truth;
- We forgo with accurate noise modelling and propose reconstruction using a novel type of fidelity based on confidence intervals (treated as bounds in a partial order).

Reconstruction based on Order Intervals

Suppose that (pointwise) error bounds for the data are available:

$$s_i^l(x) \leqslant s_i(x) \leqslant s_i^u(x) \quad \text{a.e.}, \quad i = 0, 1, \ldots, N.$$

Bounds preserved under the monotone $\log(\cdot)$ transformation:

$$g_i^l(x) = \log \frac{s_i^l(x)}{s_0^u(x)} \leqslant \langle b_i \otimes b_i, u(x) \rangle \leqslant \log \frac{s_i^u(x)}{s_0^l(x)} = g_i^u(x) \text{ a.e.}, \quad i = 1, \ldots, N.$$

Reconstruction based on Order Intervals

Suppose that (pointwise) error bounds for the data are available:

$$s_i^l(x) \leqslant s_i(x) \leqslant s_i^u(x) \quad \text{a.e.,} \quad i = 0, 1, \ldots, N.$$

Bounds preserved under the monotone $\log(\cdot)$ transformation:

$$g_i^l(x) = \log \frac{s_i^l(x)}{s_0^u(x)} \leqslant \langle b_i \otimes b_i, u(x) \rangle \leqslant \log \frac{s_i^u(x)}{s_0^l(x)} = g_i^u(x) \text{ a.e.,} \quad i = 1, \ldots, N.$$

Linear reconstruction using error bounds

$$\min_u \; R(u) \quad \text{subject to} \quad \begin{array}{l} u \geqq 0, \\ g_i^l \leqslant A_i u \leqslant g_i^u, \quad i = 1, \ldots, N, \end{array}$$

where $[A_i u](x) := \langle b_i \otimes b_i, u(x) \rangle$.

Reconstruction based on Order Intervals

Suppose that (pointwise) error bounds for the data are available:

$$s_i^l(x) \leqslant s_i(x) \leqslant s_i^u(x) \quad \text{a.e.,} \quad i = 0, 1, \ldots, N.$$

Bounds preserved under the monotone $\log(\cdot)$ transformation:

$$g_i^l(x) = \log \frac{s_i^l(x)}{s_0^u(x)} \leqslant \langle b_i \otimes b_i, u(x) \rangle \leqslant \log \frac{s_i^u(x)}{s_0^l(x)} = g_i^u(x) \text{ a.e.,} \quad i = 1, \ldots, N.$$

Linear reconstruction using error bounds

$$\min_u \ R(u) \quad \text{subject to} \quad \begin{array}{l} u \geqq 0, \\ g_i^l \leqslant A_i u \leqslant g_i^u, \quad i = 1, \ldots, N, \end{array}$$

where $[A_i u](x) := \langle b_i \otimes b_i, u(x) \rangle$.

What's the theory behind this ?

Layout

Banach Lattices[3]

- A vector space X endowed with a partial order relation $\leqslant$ is called an *ordered vector space* if

$$x \leqslant y \implies x + z \leqslant y + z \qquad \forall\ x, y, z \in X,$$
$$x \leqslant y \implies \lambda x \leqslant \lambda y \qquad \forall\ x, y \in X \text{ and } \lambda \in \mathbb{R}_+.$$

- If the partial order $\leqslant$ is a lattice, i.e.

$$\forall x, y \in X \quad \exists\, x \vee y \in X,$$

  then X is called a *vector lattice* (or a *Riesz space*).

$$x \vee 0 = x_+, \quad (-x)_+ = x_-, \quad x = x_+ - x_-, \quad |x| = x_+ + x_-.$$

- If a vector lattice X is equipped with a monotone norm, i.e.

$$\forall x, y \in X \quad |x| \geqslant |y| \implies \|x\| \geqslant \|y\|,$$

  then X is called a *Banach lattice* (if X is norm complete).

[3] H. Schaefer. Banach Lattices and Positive Operators, Springer, 1974

Error Modeling in Banach Lattices

Equation:

$$Ax = y, \quad x \in X,\, y \in Y,$$

where X, Y are Banach lattices, A is a regular operator.

Error bounds:

$$\begin{aligned}
&y_n^l \colon y_{n+1}^l \geqslant y_n^l, && A_n^l \colon A_{n+1}^l \geqslant A_n^l,\\
&y_n^u \colon y_{n+1}^u \leqslant y_n^u, && A_n^u \colon A_{n+1}^u \leqslant A_n^u,\\
&y_n^l \leqslant y \leqslant y_n^u, && A_n^l \leqslant A \leqslant A_n^u \quad \forall\, n \in \mathbb{N},\\
&\|y_n^u - y_n^l\| \to 0, && \|A_n^u - A_n^l\| \to 0 \quad \text{as } n \to \infty.
\end{aligned}$$

Feasible set:

$$X_n = \{x \geqslant 0 \colon A_n^l x \leqslant y_n^u,\ A_n^u x \geqslant y_n^l\}.$$

Theorem

Let

$$x_n = \arg\min_{x \in X_n} \mathcal{R}(x).$$

If

- $\mathcal{R}(x)$ *is bounded from below on* X*,*
- $\mathcal{R}(x)$ *is lower semi-continuous on* X*,*
- *the level-sets* $\{x \colon \mathcal{R}(x) \leqslant C\}$ *are strong compacts in* X*,*

then $\|x_n - \bar{x}\| \to 0$ *and* $\mathcal{R}(x_n) \to \mathcal{R}(\bar{x})$*.*

[4] Y.K. (2014) *Making use of a partial order in solving inverse problems: II*, Inv. Probl. 30, 085003

Our Choice of the Regulariser: Total Generalised Variation[5]

Total Generalised Variation is a higher-order extension of Total Variation. It turns out that the standard BV norm

$$\|u\|_{\mathrm{BV}(\Omega;\mathrm{Sym}^k(\mathbb{R}^m))} := \|u\|_{L^1(\Omega;\mathrm{Sym}^k(\mathbb{R}^m))} + \mathrm{TV}(u)$$

and the "BGV norm"

$$\|u\|' := \|u\|_{L^1(\Omega;\mathrm{Sym}^k(\mathbb{R}^m))} + \mathrm{TGV}^2_{(\beta,\alpha)}(u)$$

are topologically equivalent norms on $\mathrm{BV}(\Omega;\mathrm{Sym}^k(\mathbb{R}^m))$, yielding the same convergence results for TGV and TV regularisation.

If the L_1-norm of u is bounded a priori then the level sets $\{u\colon \mathrm{TGV}^2_{(\beta,\alpha)}(u) \leqslant C\}$ are strong compacts in $L_1(\Omega;\mathrm{Sym}^k(\mathbb{R}^m))$.

[5] Bredies, Kunisch, Pock (2011). *Total generalized variation*, SIAM J. Imaging Sci. 3, 492-526

Error Bounds Derived from Data

- Pointwise error bounds in the data may not be directly available
- attempt to use confidence intervals as pointwise bounds, i.e. to find for each true signal f individual *random* upper and lower bounds $\hat{f}^u$ and $\hat{f}^l$ such that

$$P(\hat{f}^u \leq f \leq \hat{f}^l) = 1 - \theta$$

- In the i-th voxel, the measured value $\hat{f}^i$ is the sum of the true value f^i and additive noise ν^i:

$$\hat{f}^i = f^i + \nu^i$$

- all ν^i assumed i.i.d., but their distribution is unknown
- background regions with zero mean ($f_i = 0$) provide us with a number of independent samples from the unknown distribution of ν, which can be used to estimate this distribution.

Layout

Test Case with Synthetic Data

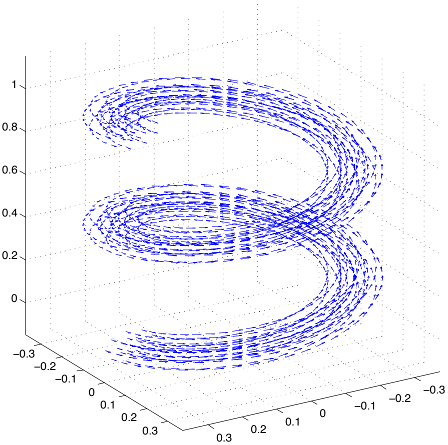

Figure: The principal eigenvector field of the ground-truth tensorfield

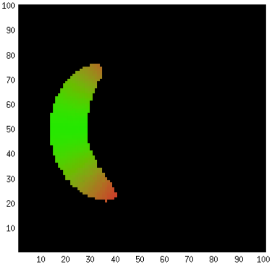

(a) Ground truth

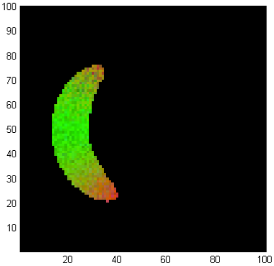

(b) No regularisation

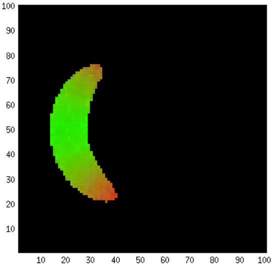

(c) L_2-nonlin (discr. pr.)

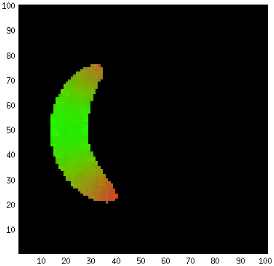

(d) L_2-linear (discr. pr.)

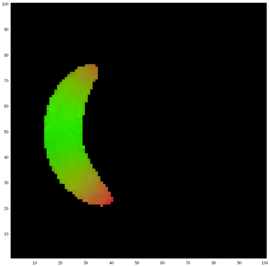

(e) Err. bounds (95%)

We plot the colour-coded principal eigenvector with intensity modulation by fractional anisotropy.

Numerical results for the synthetic data

Table: For the L^2 and non-linear L^2 reconstruction models the ‘free parameter’ is the regularisation parameter α, and for the error bounds approach it is the confidence interval.

Method	Parameter choice	Frobenius PSNR	Pr. e.val. PSNR	Pr. e.vect. angle PSNR
Regression		33.90dB	25.04dB	47.86dB
Linear L^2	Discr. Principle	32.93dB	27.81dB	61.89dB
Linear L^2	Frob. Error-optimal	34.51dB	28.42dB	60.93dB
Non-linear L^2	Discr. Principle	37.33dB	27.81dB	61.89dB
Non-linear L^2	Frob. Error-optimal	37.44dB	28.03dB	61.12dB
Err. bounds	90%	32.28dB	28.86dB	65.65dB
Err. bounds	95%	30.97dB	28.14dB	64.80dB
Err. bounds	99%	27.86dB	24.51dB	61.41dB

Errors in Fractional Anisotropy

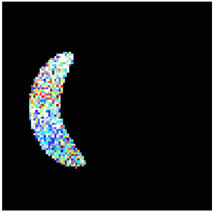

(a) Regr. result

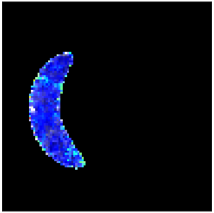

(b) L^2-linear, discr. pr.

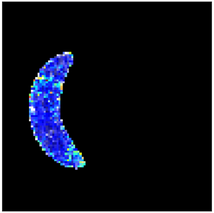

(c) L^2-linear, error-optimal

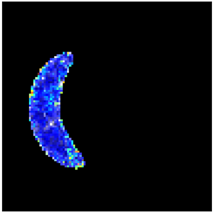

(d) L^2-nonlin, discr. pr.

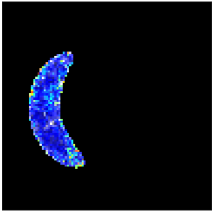

(e) L^2-nonlin, error-optimal

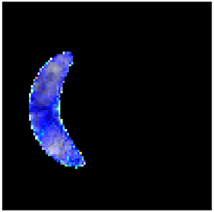

(f) Err. bounds, 95% conf. int.

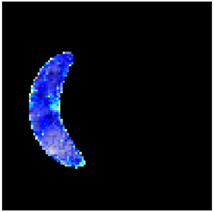

(g) Err. bounds, 90% conf. int.

Layout

Slice of a real MRI measurement

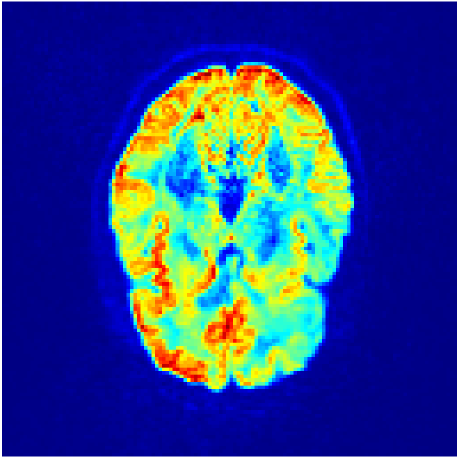

We are grateful to Karl Koschutnig for giving us access to the in vivo data set of a human brain, with the measurements of a volunteer performed on a clinical 3T system (Siemens Magnetom TIM Trio, Erlangen, Germany),

Reconstruction of Real Images

- No ground truth available, pseudo-ground-truth estimated using regression from four repeated measurements;
- Only one measurement per gradient is used for reconstruction.

Real Data: Colour-Coded Directions of the Principal Eigenvector

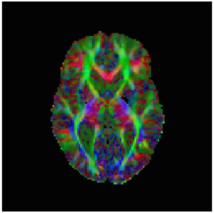

(a) Pseudo-ground-truth

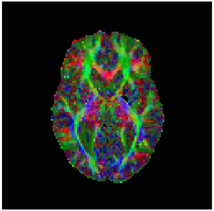

(b) Regression result

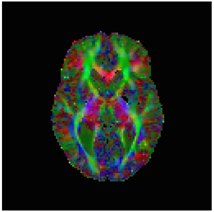

(c) Linear L^2, discr. principle

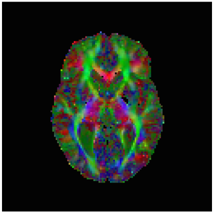

(d) Linear L^2, error-optimal

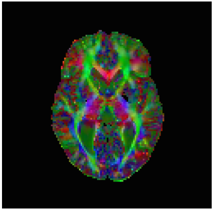

(e) Non-linear L^2, discr. principle

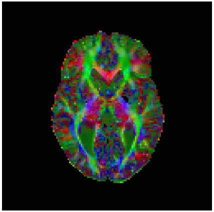

(f) Non-linear L^2, error-optimal

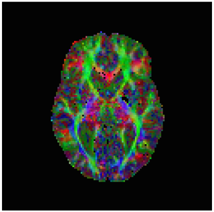

(g) Err. bounds, 95% conf. int.

Numerical results for the in-vivo brain data

Table: For the L^2 and non-linear L^2 reconstruction models the 'free parameter' is the regularisation parameter α, and for the error bounds approach it is the confidence interval.

Method	Parameter choice	Frobenius PSNR	Pr. e.val. PSNR	Pr. e.vect. angle PSNR
Regression		32.35dB	33.67dB	28.56dB
Linear L^2	Discr. Principle	34.80dB	36.35dB	24.81dB
Linear L^2	Frob. Error-optimal	34.81dB	36.32dB	24.97dB
Non-linear L^2	Discr. Principle	33.53dB	35.87dB	27.12dB
Non-linear L^2	Frob. Error-optimal	33.57dB	36.03dB	27.58dB
Err. bounds	90%	33.71dB	34.93dB	27.00dB
Err. bounds	95%	33.70dB	34.97dB	26.91dB
Err. bounds	99%	33.67dB	34.89dB	26.88dB

Fractional anisotropy of the *corpus callosum* in greyscale and principal eigenvector

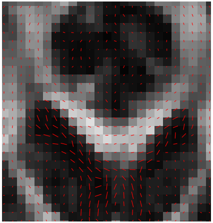

(a) Pseudo-ground-truth

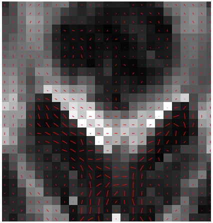

(b) Linear L^2, discr. pr.

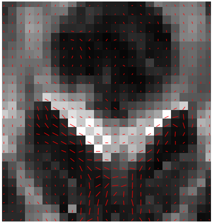

(c) Linear L^2, error-opt.

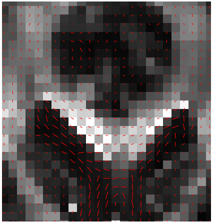

(d) Non-linear L^2, discr. pr.

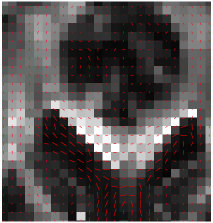

(e) Non-linear L^2, error-opt.

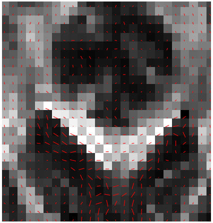

(f) Err. bounds, 95% conf. int.

Real Data: Tractography Results

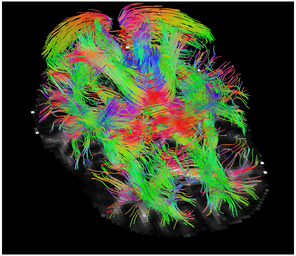

(a) Pseudo-ground-truth

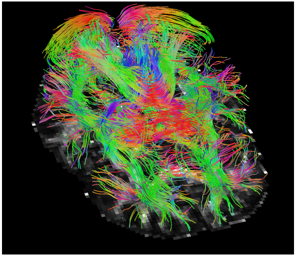

(b) Regression result

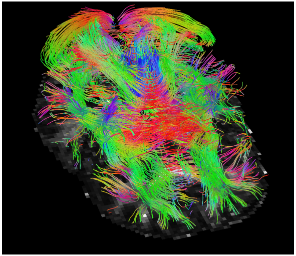

(c) Linear L^2, discr. pr.

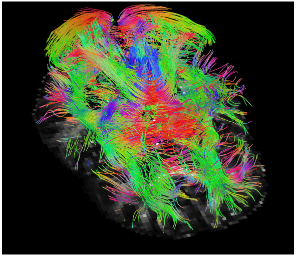

(d) Non-lin. L^2, discr. pr.

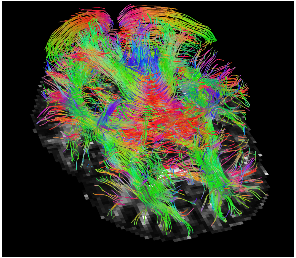

(e) Constr., 95% C.I.

Conclusions

Conclusions:

- The error bounds based approach is a feasible, distribution - independent alternative to standard modelling with incorrect Gaussian assumptions;
- Very good reconstruction of the direction of the principal eigenvector – potentially useful for tractography;
- But some problems with fractional anisotropy;
- PSNR increases as the confidence level gets smaller. Can the confidence level be used as a regularisation parameter?

Details:

- A. Gorokh, Y. Korolev, T. Valkonen (2016). *Diffusion tensor imaging with deterministic error bounds*, J. Math. Imaging Vis, 56(1), 137-157

THANK YOU FOR YOUR ATTENTION !